

Electronic supplementary information (ESI)

Topological defects due to twist-bend nematic drops mimicking colloidal particles in a nematic medium

K. S. Krishnamurthy,^{*a} D. S. Shankar Rao,^a Madhu B. Kanakala,^a Channabasaveshwar V. Yelamaggad,^a and Maurice Kleman^{*b}

¹Centre for Nano and Soft Matter Sciences, P. O. Box 1329, Jalahalli, Bangalore 560013, India

²Institut de Physique du Globe de Paris, Université de Paris, 1, rue Jussieu, 75238 Paris cedex 05, France

*E-mail: murthyksk@cens.res.in, kleman@ipgp.fr

A. Phase diagram

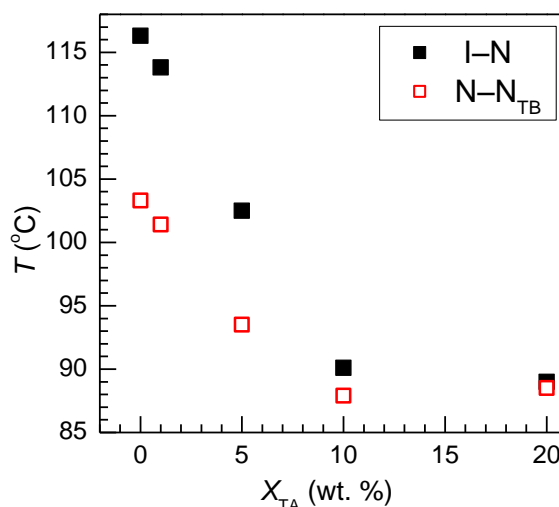


Fig. S1. Concentration X_{TA} (wt. %) of 1-tetradecanoic acid–temperature T phase diagram for the binary system CB7CB/TA, showing the isotropic (I) to nematic (N), and N to twist-bend nematic (N_{TB}) transitions determined from polarization microscopic studies. The N- N_{TB} coexistence region (not indicated) is very narrow (≤ 1 °C) in all the mixtures except M_5 in which it extends to a few °C. Around 85 °C, phase separation takes place in M_5 , with TA-rich droplets appearing dispersed sporadically in the N_{TB} -rich matrix. This separation occurs in M_{20} even at the onset of nematic phase.

B. Video clips

Note: Reference axes x and y are along the horizontal and vertical frame-edges. Relative temperature $\Delta T_r = T_B - T$, with T_B denoting the N- N_{TB} transition temperature.

(a) **V1.avi**, showing the growth of an N_{TB} drop in the nematic phase of *pure* CB7CB close to T_B (~ 103 °C), is from a series of time lapse images recorded at 6.1 fps; it runs at 10 fps. The sample was a 20 μm thick layer in a planar cell (rubbing axis x), viewed in white light, between crossed polarizers P(0)–A(90), set along (x, y) .

(b) **V2.avi**, from a time lapse image series recorded at 0.85 fps, runs at 2 fps. It shows the morphology of N_{TB} domains growing in the N phase; $\Delta T_r = 0.5$ °C. The sample is a 20 μm thick layer of the mixture M_5 (5 wt. % TA/CB7CB) in a planar cell, viewed between diagonally crossed polarizers P(45)–A(135). N_{TB} domains appearing at the onset as tactoid-like drops (in plan view) transform into radial hedgehogs through a series of structural modifications. With counter hedgehogs induced in the enveloping nematic, dipoles and their doublets are generated. N_{TB} dimers exhibit facile rotation around the layer normal z , tending to align along the far field N director \mathbf{n}_0 .

(c) **V3.avi**, from a time lapse image series recorded at 0.2 fps, runs at 2 fps. It shows the elastic propulsion of one of the two nearly parallel dipoles on the left toward the antiparallel dipole to the right in a 20 μm thick sample of M_5 , held in a 90° twist cell, at $\Delta T_r=0.3^\circ\text{C}$, and viewed between parallel polarizers P(0)–A(0).

(d) **V4.avi**, recorded at 0.88 fps, runs at 10 fps. It shows the transition of a hyperbolic hedgehog into a Saturn ring, in a 20 μm thick layer of M_5 in a planar alignment cell; $\Delta T_r=1.8^\circ\text{C}$. Crossed polarizers P(0)–A(90).

(d) **V5.avi**, recorded at 3.5 fps, runs at 7 fps. It shows the final stages of transition of a Saturn ring defect, progressively drifting to the left, into a hyperbolic hedgehog, in a 20 μm thick layer of M_5 in a planar alignment cell; $\Delta T_r\approx 1^\circ\text{C}$. Crossed polarizers P(0)–A(90). The drop is $\sim 24\ \mu\text{m}$ in diameter initially.

(e) **V6.avi**, showing a Saturn ring defect is from z -stacked images recorded at 1 μm interval, using laser scanning microscopy (with a He-Ne 543 nm beam). It runs at 5 fps. Sample is a 20 μm thick layer of M_5 in a planar cell at $\Delta T_r=0.4^\circ\text{C}$, held between crossed Polarizers, P(0)–A(90).

(f) **V7.avi**, showing the transformation of a hyperbolic hedgehog into a hybrid disclination ring, is from time images recorded at 0.48 fps; it runs at 1 fps. Sample is a 20 μm thick layer of M_5 in a 90° twist cell at $\Delta T_r=1^\circ\text{C}$, held between parallel Polarizers, P(0)–A(0). The figure-of-eight-shaped white line defect around the N_{TB} drop consists of twist and $-1/2$ wedge segments.

(g) **V8.avi**, showing the coalescence of two N_{TB} drops and simultaneous transformation of -1 counter defects into a twisted hybrid ring, is from time images recorded at 0.2 fps; it runs at 7 fps. Sample is a 20 μm thick layer of M_5 in a 90° twist cell; $\Delta T_r=0.7^\circ\text{C}$; Polarizers held initially parallel along x [P(0)–A(0)], are switched midway to the crossed position P(90)–A(0).

C. Dipoles in pure CB7CB

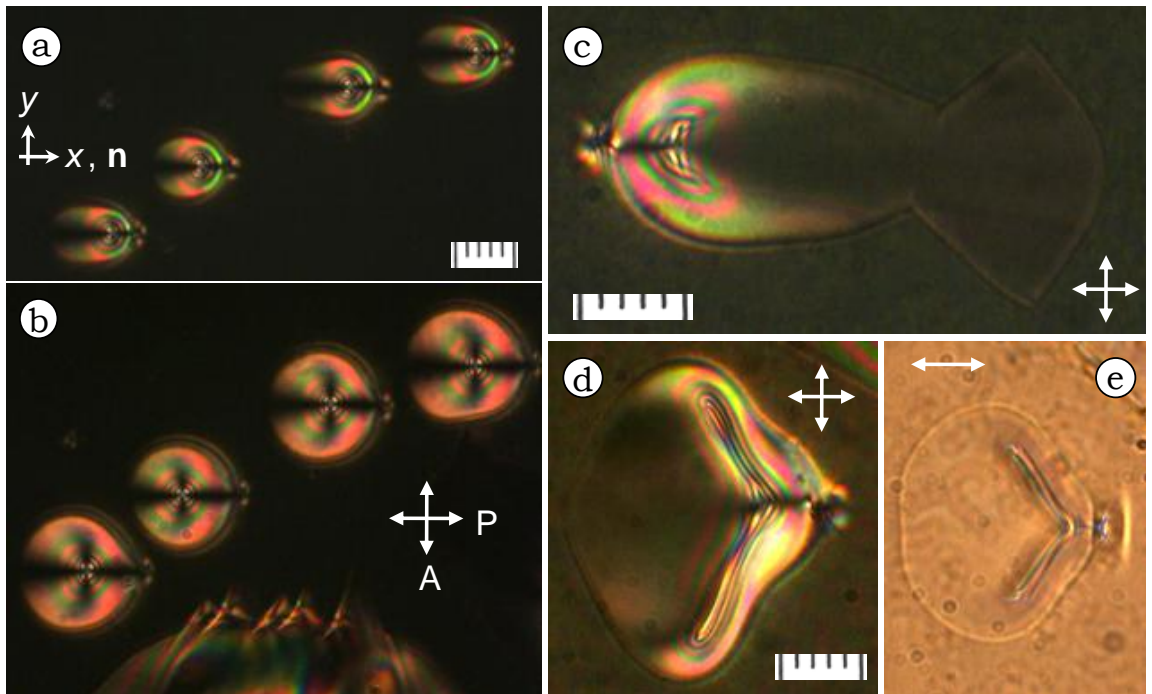


Fig. S2. N_{TB} droplets formed in *pure* CB7CB in the narrow N – N_{TB} coexistence region with the radial hedgehog geometry generate companion hyperbolic hedgehogs of the nematic. (a) Some parallel dipoles oriented along $-x$; (b) in plan view, N_{TB} drops appearing oblong in (a) assume, as they grow, a circular shape; competing N_{TB} domains of a different morphology, seen at lower edge in (b), nucleate and grow at the expense of dipolar domains. (c) A tactoidlike domain coupled to an N_{TB} radial hedgehog. (d) and (e) Changing shape of the N_{TB} drop with fingerlike new structural defects developing in them. $\Delta T_r=0.4^\circ\text{C}$. Sample thickness $d=20\ \mu\text{m}$. Planar alignment cell; nematic far-field director \mathbf{n} along x . Scale: 5 μm each subdivision.

D. Knotted N_{TB} drops

Note: The figures S3-S8 below pertain to the textures observed in the N - N_{TB} coexistence region of a $20\ \mu\text{m}$ thick layer of the mixture M_5 in a 90° twist cell. Reference axes as in Fig. S2.

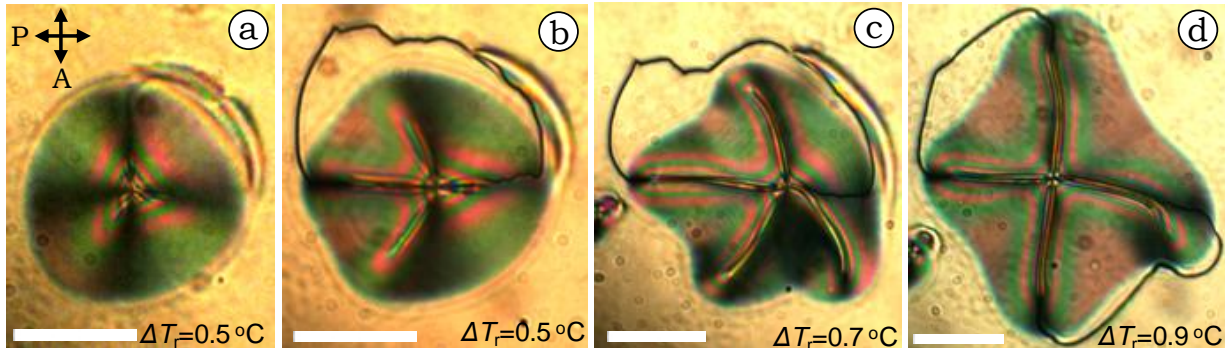


Fig. S3 Hyperbolic hedgehog to Saturn ring two-step-transformation process in a $20\ \mu\text{m}$ thick M_5 layer held in a 90° twist cell. (a) A dipole oriented along a diagonal; the top radial dark line is a part of the developing loop that eventually, over a few minutes, takes the geometry in (b). The loop in (b) involves a horizontal-looking $-1/2$ disclination segment and a twist line segment lying outside the drop; the twist line connects to the partly decayed -1 hedgehog. On reducing the temperature by $0.2\ ^\circ\text{C}$, the drop enlarges and the focal line defects within it grow; but the transformation remains (during 1 h wait) half completed. Soon after reducing the temperature by $0.2\ ^\circ\text{C}$ more, the part-hedgehog fuses completely and the figure-of-eight knot appears. Scale bar: $20\ \mu\text{m}$.

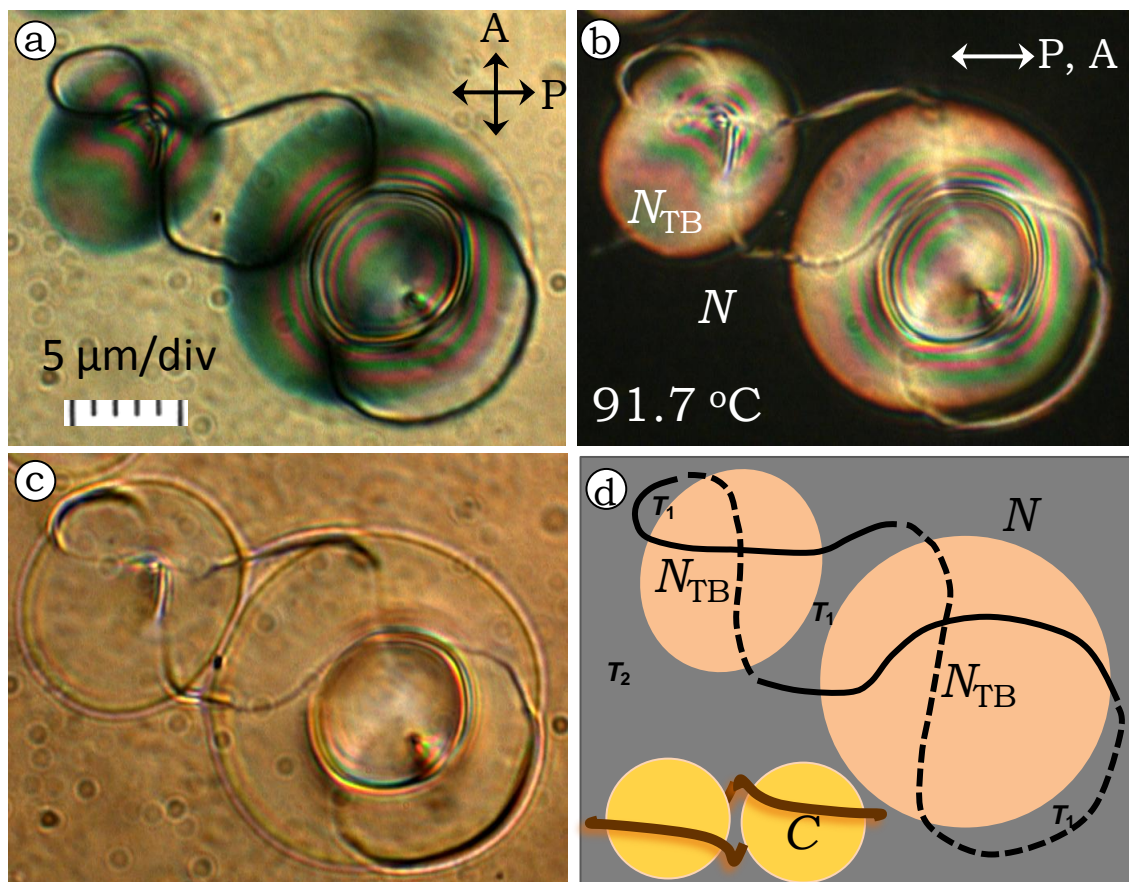


Fig. S4. (a-c) Figure-of-eight knot binding two N_{TB} drops in a $20\ \mu\text{m}$ thick M_5 layer, between orthogonally rubbed plates. In the bigger drop, the radial hedgehog has opened out into a $+1/2$ ring. (d) Schematic of the disclination loop in which the continuous black line passes above the dashed line. The corresponding topological defect configuration for dimeric solid colloidal particles C is at bottom left (see ESI ref. 1).

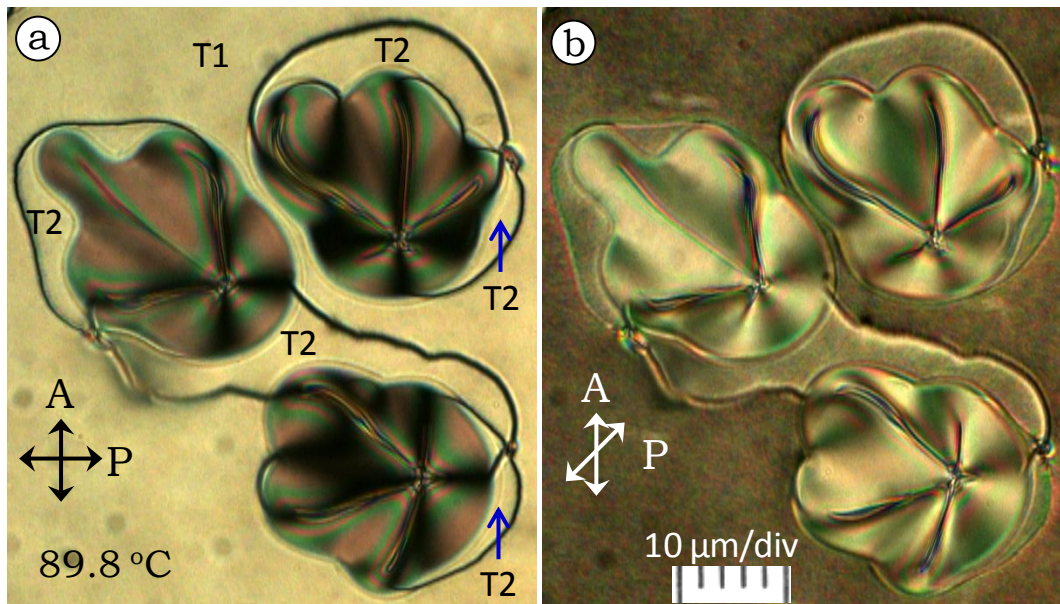


Fig. S5. Dipolar defects due to N_{TB} drops of M_5 , dispersed in the 90° twisted nematic matrix of the same mixture; the drops, acting as +1 hedgehogs, have produced *transient* counterpoint defects in the nematic; two of the dipoles are antiparallel and coupled, and separated from the third; the -1 hedgehogs, still undergoing transformation into line defects, are all in their final stages of decay. T1 and T2 are oppositely twisted nematic regions; the difference in their interference contrast is evident in (b). The radiating focal line defects within the drops are possibly due to pairs of disclinations to which are attached pairs of screw dislocations.

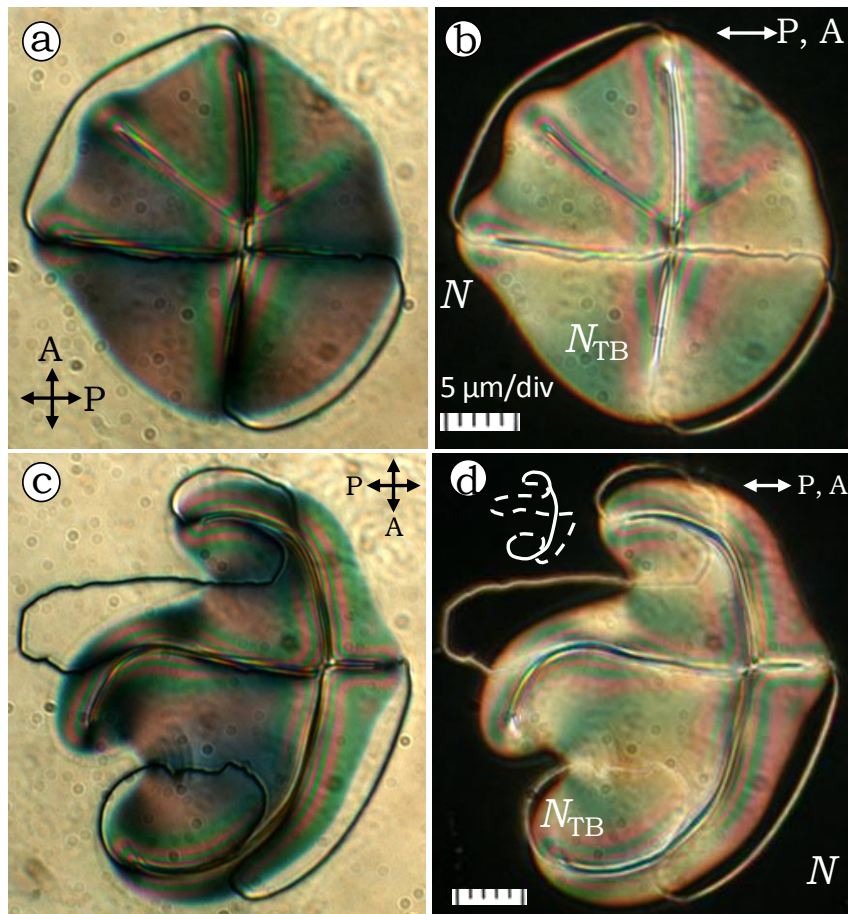


Fig. S6. (a, b) An N_{TB} drop with a figure of eight disclination loop around it; additional line defects radiating from the centre are the focal lines; they seem to involve pairs of disclinations to which are attached pairs of screw dislocations. (c, d) The N_{TB} drop here has prominent fingerlike extensions, which are involved in the loop surrounding it. The inset in (d) shows is a schematic of the loop, with the continuous line segment above the dashed segment.

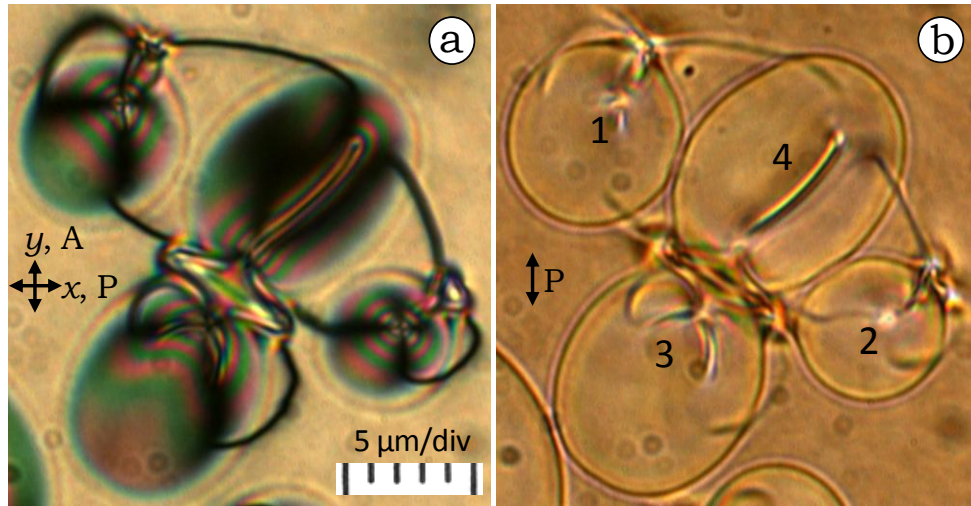


Fig. S7. Entanglement of four N_{TB} drops by a network of disclination lines. The hyperbolic point defects due to hedgehogs 1 and 2 have not fully transformed into Saturn ring segments. The hedgehogs generated by drops 3 and 4 have apparently fused to form what may be analogous to the so-called bubblegum configuration in colloidal chiral nematics (see ESI ref. 2).

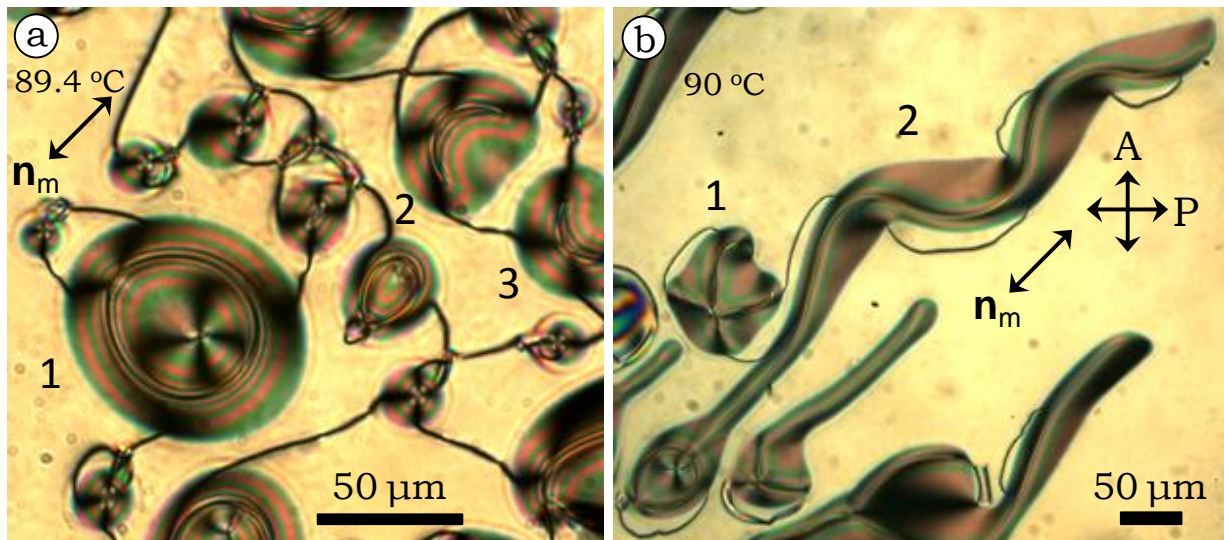


Fig. S8. (a) A large number of N_{TB} drops interlinked essentially by twist lines, seen against quarter turn twisted N background. But for a few large drops (1-3), all others have the hyperbolic defects persisting, with the dipoles along the midplane director n_m . (b) Some N_{TB} drops grow sinusoidally along n_m to great lengths at lower temperatures. Note that drop 1, which has no -1 point defect remaining, is surrounded by a wedge-twist hybrid line that links to the diagonal wavy extension of the drop below. The horizontal and vertical sections of the diagonal domain 2 are connected by twist lines.

E. The Frank-Pryce configuration

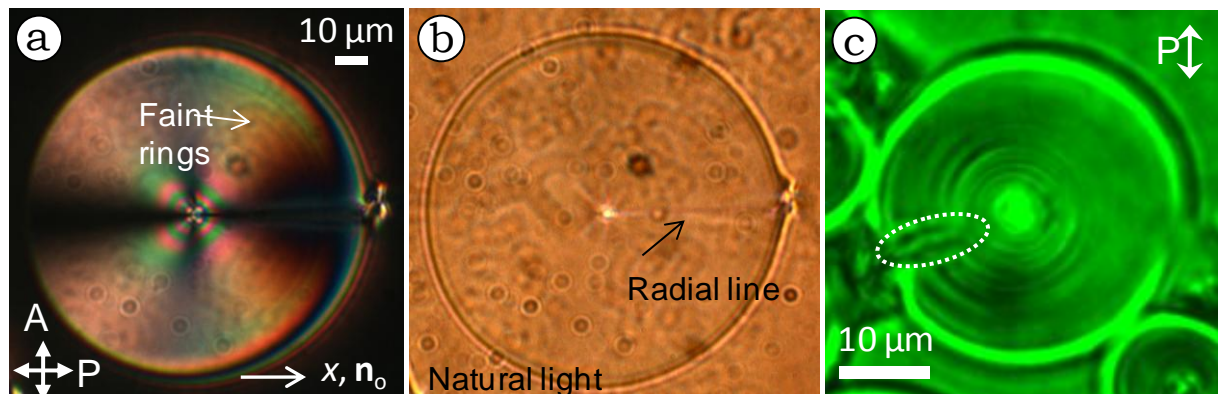


Fig. S9. (a) A large, circular N_{TB} drop with the geometry of a radial hedgehog showing faint rings and a radial line defect between its centre and the hyperbolic hedgehog. The central color fringes are triangular, unlike what is expected for spherical pseudo layers. The interaction of charges seems to alter the circular symmetry of birefringence bands. (b) Same drop as in (a), viewed in ordinary light. (c) Image of an N_{TB} drop in a 90° twist cell obtained using a green filter, showing a fuzzy radial line and several concentric rings.

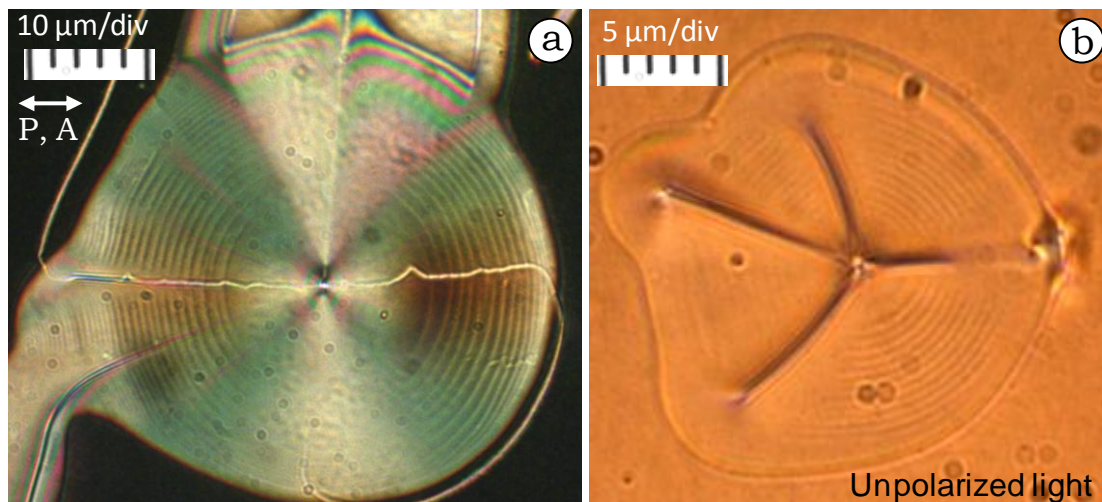


Fig. S10 Large N_{TB} drops showing regular fringes; the surrounding nematic matrix is 90° twisted planar in (a) and untwisted planar in (b). The central part of the drops is uniform; hence the fringes in the outer region are due to the wedge like geometry of the drops therein. The origin of the modulation could be due to one of the following: (i) two-beam interference, (ii) chirality, (iii) concentration gradient and (iv) microscale undulations. Samples are $20\ \mu\text{m}$ thick M_5 layers.

ESI References

- 1 S. Žumer, I. Muševič, M. Ravnik, M. Škarabot, I. Poberaj, D. Babič and U. Tkalec, *Proc. of SPIE*, 2008, **6911**, 69110C.
- 2 U. Tkalec, M. Ravnik, S. Žumer and I. Muševič, *Phys. Rev. Lett.*, 2009, **103**, 127801.